Supporting Information

Zheng, Y. et al, "Lipoxygenases mediate the effect of essential fatty acid in skin barrier formation: A proposed role in releasing omega-hydroxyceramide for construction of the corneocyte lipid envelope"

Additional Experimental Procedures

HPLC conditions for the Main Text Figures:

Fig. 2A: Column: Zorbax Eclipse XDB-C8 column (5 μm, 4.6 mm × 15 cm). Solvent: methanol/hexane (10:1, v/v). Flow rate: 1 ml/min.
Fig. 2C: [Left panel] Column: Beckman Silica Ultrasphere column (5 μm, 4.6 mm × 25 cm). Solvent: hexane/isopropanol (100:1.5, v/v). Flow rate: 1 ml/min. [Right panel] Column: Chiralpak AD column (5 μm, 4.6 mm × 25 cm). Solvent: hexane/methanol/ethanol (100:5:5 v/v/v). Flow rate: 1ml/min.
Fig. 2D: Column: Beckman Silica Ultrasphere column (5 μm, 4.6 mm × 25 cm). Solvent: hexane/isopropanol (100:2, v/v). Flow rate: 1 ml/min.

Fig. 3A: Column: Beckman Silica Ultrasphere column (5 μm, 4.6 mm × 25 cm). Solvent: hexane/isopropanol/acetic acid (90:10:0.1, v/v/v). Flow rate: 1 ml/min.
Fig. 3B: [Left panel] Column: Beckman Silica Ultrasphere column (5 μm, 4.6 mm × 25 cm). Solvent: hexane/isopropanol (100:2, v/v). Flow rate: 1 ml/min. [Right panel] Column: Chiralpak AD column (5 μm, 4.6 mm × 25 cm). Solvent: hexane/methanol/ethanol (100:5:5 v/v/v). Flow rate: 1ml/min.
Fig. 3C: [Left panel] Column: Beckman Silica Ultrasphere column (5 μm, 4.6 mm × 25 cm). Solvent: hexane/isopropanol (100:2, v/v). Flow rate: 1 ml/min. [Right panel] Column: Chiralpak AD-H column (5 μm, 2.1 mm × 15 cm). Solvent: hexane/methanol/ethanol (100:5:5 v/v/v). Flow rate: 0.3 ml/min.

Fig. 4A,B: Column: Beckman Silica Ultrasphere column (5 μm, 4.6 mm × 25 cm). Solvent: hexane/isopropanol/acetic acid (90:10:0.1, v/v/v). Flow rate: 1 ml/min. (A) Injected was 5% of the total extract of free ceramides from the epidermis of one neonatal (P0) mouse (wild-type or 12*R*-LOX-/-). (B) Injected was 25% of the total extract from the first cycle of room temperature overnight soak of the protein pellet from the epidermis of one neonatal (P0) mouse.
Fig. 4D: [Left panel] Column: Beckman Silica Ultrasphere column (5 μm, 4.6 mm × 25 cm). Solvent: hexane/isopropanol (100:1.5, v/v). Flow rate: 1 ml/min. [Right panel] Column: Chiralpak AD-H column (5 μm, 2.1 mm × 15 cm). Solvent: hexane/methanol/ethanol (100:5:5 v/v/v). Flow rate: 0.3 ml/min.

Fig. 5A,B: [Left panel] Column: Waters Symmetry C18 column (5 μm, 4.6 mm × 25 cm). Solvent: methanol/water/acetic acid (80:20:0.01, v/v/v). Flow rate: 1 ml/min. [Middle panel] Column: Beckman Silica Ultrasphere column (5 μm, 4.6 mm × 25 cm). Solvent: hexane/isopropanol (100:2:0.02, v/v/v). Flow rate: 1 ml/min. [Right panel] Column: Chiralpak

AD column (5 μm, 2.1 mm × 15 cm). Solvent: hexane/methanol/ethanol/acetic acid (100:5:5/0.02 v/v/v/v). Flow rate: 0.2 ml/min.

Fig. 6B,C: Column: Beckman Silica Ultrasphere column (5 μm, 4.6 mm × 25 cm). Solvent: hexane/isopropanol/acetic acid (90:10:0.1, v/v/v). Flow rate: 1 ml/min. Injected was 2% of the total extract of the ester-linked protein-bound lipids from the epidermis of one neonatal (P0) mouse (wild-type or 12*R*-LOX-/-).

HPLC conditions for the Supplemental Figures

Supplemental Fig. S1A: Column: Beckman Silica Ultrasphere column (5 μm, 4.6 mm × 25 cm). Solvent: hexane/isopropanol/acetic acid (90:10:0.1, v/v/v). Flow rate: 1 ml/min.
Fig. S1B: [Left panel] Column: Beckman Silica Ultrasphere column (5 μm, 4.6 mm × 25 cm). Solvent: hexane/isopropanol (100:2, v/v). Flow rate: 1 ml/min. [Right panel] Column: Chiralpak AD column (5 μm, 4.6 mm × 25 cm). Solvent: hexane/methanol/ethanol (100:5:5 v/v/v). Flow rate: 1ml/min.
Fig. S1C,D: Column: Beckman Silica Ultrasphere column (5 μm, 4.6 mm × 25 cm). Solvent: hexane/isopropanol (100:2, v/v). Flow rate: 1 ml/min.

Supplemental Fig. S2B: Column: Beckman Silica Ultrasphere column (5 μm, 4.6 mm × 25 cm). Solvent: hexane/isopropanol (100:0.5, v/v). Flow rate: 1 ml/min.

Supplemental Fig. S3A,B: [Left panel] Column: Beckman Silica Ultrasphere column (5 μm, 4.6 mm × 25 cm). Solvent: hexane/isopropanol (100:1.5, v/v). Flow rate: 0.5 ml/min. [Right panel] Column: Chiralpak AD column (5 μm, 2.1 mm × 15 cm). Solvent: hexane/methanol/ethanol (100:5:4 v/v/v). Flow rate: 0.2 ml/min.

Supplemental Fig. S4: Column: Beckman Silica Ultrasphere column (5 μm, 4.6 mm × 25 cm). Solvent: hexane/isopropanol/acetic acid (90:10:0.1, v/v/v). Flow rate: 1 ml/min. (**A**) and (**B**): Injected was 1% of the total extract of free ceramides from the epidermis of one neonatal (P0) mouse (wild-type or 12*R*-LOX-/-). (**C**) Injected was 20% of the total extract from the first cycle of room temperature overnight soak of the protein pellet from the epidermis of one neonatal (P0) mouse.

Supplemental Fig. S5: Column: Beckman Silica Ultrasphere column (5 μm, 4.6 mm × 25 cm). Solvent: hexane/isopropanol/acetic acid (90:10:0.1, v/v/v). Flow rate: 1 ml/min.

Supplemental Fig. S6A,B: Column: Waters Symmetry C18 column (5 μm, 2.1 mm × 15 cm). Solvent: methanol/acetic acid (100:0.01, v/v). Flow rate: 0.2 ml/min. Injected was 7% of the total extract of the ester-linked protein-bound lipids from the epidermis of one neonatal (P0) mouse (wild-type or 12*R*-LOX-/-)

Legends to Supporting Figures

Fig. S1: Transformation of EOS by 12*R*-LOX and eLOX3 *in vitro*. (**A**) SP-HPLC analysis of the oxygenation of EOS by 12*R*-LOX. (**B**) SP-HPLC analysis (left panel) and chiral HPLC (right panel) of the reduced and transesterified 12*R*-LOX products as methyl esters. (**C**) SP-HPLC analysis of the transesterified products from reaction of eLOX3 with 9*R*-HPODE-EOS (the 12*R*-LOX products in panel A). (**D**) SP-HPLC analysis of the products from reaction of eLOX3 with 9*R*-HPODE methyl ester. The major product in this reaction has been identified by GC-MS and NMR as methyl 9*R*,10*R*-epoxy-13*R*-hydroxy-octadeca-11*E*-enoate. (**E**) Combined mass spectrum of the EOS substrates. (**F**) Combined mass spectrum of the 12*R*-LOX products after triphenylphosphine reduction. (**G**) Combined mass spectrum of the eLOX3 products.

Fig. S2: Analysis of oxygenated EOS metabolites from pig epidermis. (**A**) [Top panel] Combined mass spectrum of EOS. [Bottom panel] Combined mass spectrum of epOH-EOS. (**B**) SP-HPLC analysis of KODE methyl esters transesterified from KODE-EOS. (**C**) GC-MS analysis of the TMS derivative of the major epOH methyl ester transesterified from epOH-EOS. For interpretation of the prominent ions, see Fig. S1E.

Fig. S3: Analysis of transesterified oxygenated EOS metabolites (HODE-EOS and KODE-EOS) from wild-type mouse epidermis (**A**) and from 12*R*-LOX-/- mouse epidermis (**B**). SP-HPLC analysis of KODE and epOH methyl esters tranesterified from the LOX product peak shown in Fig. 4A. Note that very little epoxy-ketone was recovered due to its instability under the alkaline conditions used for transesterification. 9-HODE methyl ester was collected and further analyzed by chiral HPLC (right panel). Identical aliquots were injected in this wild-type vs. 12*R*-LOX-/- comparison. Shown are representative chromatograms from three independent experiments on the same aliquots of the extract from three sets of wild-type and 12*R*-LOX-/- littermates.

Fig. S4: Analysis of free and reversibly bound lipids from mouse epidermis. (**A**) and (**B**): Total ion current of SP-HPLC-APCI-MS analysis of free ceramides from wild-type and 12*R*-LOX-/- mouse epidermis respectively. The same aliquot was injected in this wild-type vs. 12*R*-LOX-/- comparison. (**C**) Total ion current of SP-HPLC-APCI-MS analysis of reversibly bound epoxy-ketone-EOS from wild-type mouse epidermis. (**D**) Total ion current of RP-HPLC-ESI-MS analysis of reversibly bound epoxy-ketone acyl acid from wild-type mouse epidermis. (**E**) Mass spectrum of EOS from mouse epidermis. (**F**) Mass spectrum of free epoxy-ketone-EOS from mouse epidermis. **(G)** Mass spectrum of free epOH-EOS from mouse epidermis. Note the pattern similarity between this spectrum and the spectrum of free epoxy-ketone-EOS in (**F**). (**H**) Mass spectrum of reversibly bound epoxy-ketone-EOS from mouse epidermis. (**I**) Mass spectrum of reversibly bound epoxy-ketone acyl acid from mouse epidermis.

Fig S5: Stepwise extraction of mouse epidermis reveals lipids reversibly bound to proteins. (**A**)-(**D**): First to fourth sonication and extraction by chloroform:methanol (1:1 for A and B, or 2:1 for C and D, v/v) at 0 °C. Sonication lasted for 20 min each time (20 s sonication followed by 20 s interval). After each extraction, the organic phase was removed from the protein pellet by centrifugation. (**E**): A final soak of the protein pellet in chloroform:methanol (1:1, v/v) at room temperature overnight. For the first extraction, 3% of total extract was injected onto HPLC; for the next four extractions, 25% of total extract was injected. This experiment used epidermis isolated from two neonatal (P0) BALB/c mice.

Fig. S6: Analysis of covalently bound FA and ω-hydroxy VLFA from mouse epidermis. (**A**) and (**B**): Total ion current of RP-HPLC-ESI-MS analysis of covalently bound lipids from wild-type and 12*R*-LOX-/- mouse epidermis respectively. The covalently bound lipids was recovered from mild alkaline hydrolysis of exhaustively extracted protein pellets. (**C**) Combined mass spectra of ω-hydroxy VLFA from wild-type epidermis.

Last page of Supplemental data:
Table S1: ^{1}H-NMR spectrum of 9*R*,10*R*-trans-epoxy-10*E*-13*R*-hydroxy-octadecenoate methyl ester.

Figure S1

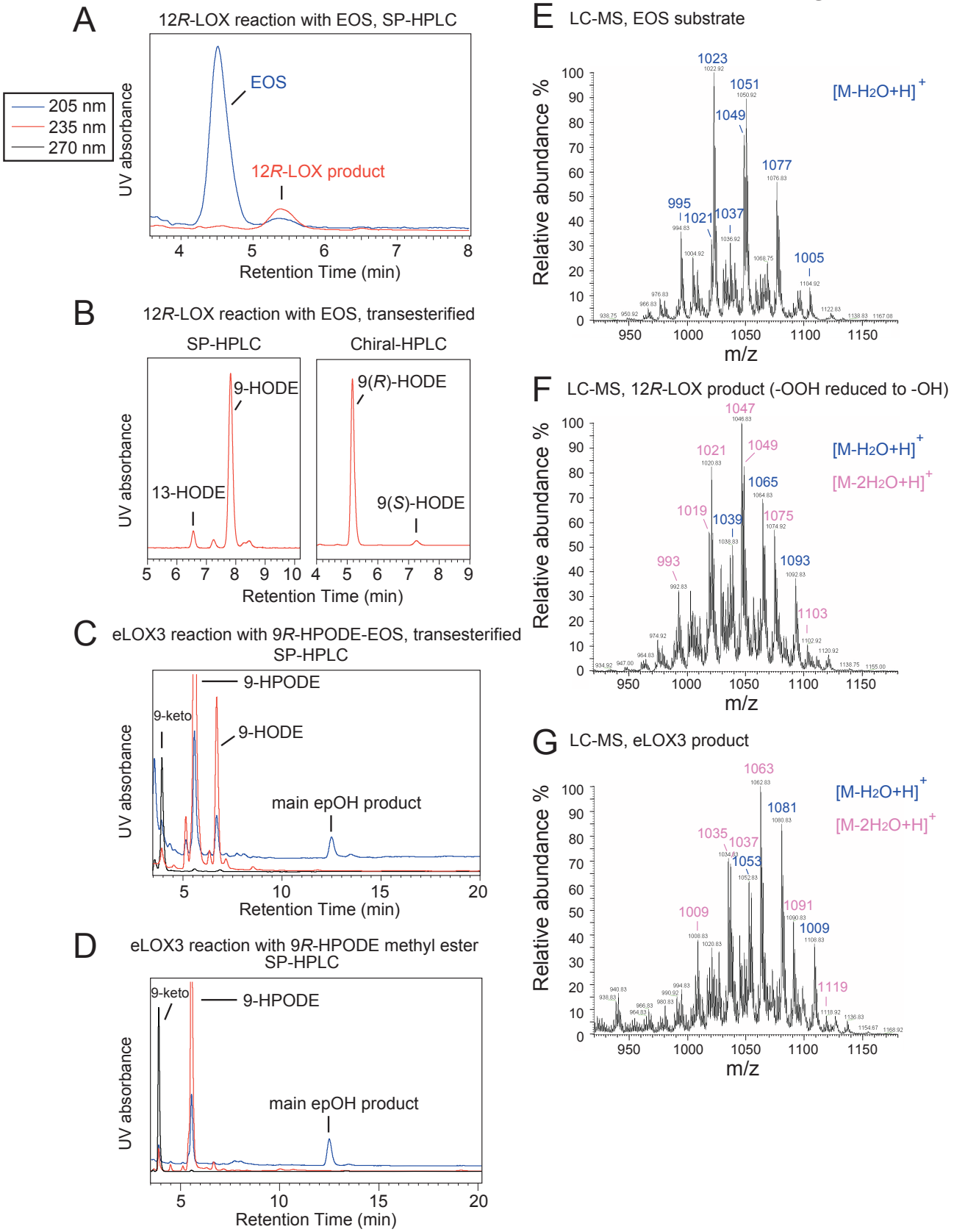

Fig. S1: Transformation of EOS by 12R-LOX and eLOX3 in vitro. (**A**) SP-HPLC analysis of the oxygenation of EOS by 12R-LOX. (**B**) SP-HPLC analysis (left panel) and chiral HPLC (right panel) of the reduced and transesterified 12R-LOX products as methyl esters. (**C**) SP-HPLC analysis of the transesterified products from reaction of eLOX3 with 9R-HPODE-EOS (the 12R-LOX products in panel A). (**D**) SP-HPLC analysis of the products from reaction of eLOX3 with 9R-HPODE methyl ester. The major product in this reaction has been identified by GC-MS and NMR as methyl 9R,10R-epoxy-13R-hydroxy-octadeca-11E-enoate. (**E**) Combined mass spectrum of the EOS substrates. (**F**) Combined mass spectrum of the 12R-LOX products after triphenylphosphine reduction. (**G**) Combined mass spectrum of the eLOX3 products.

Figure S2

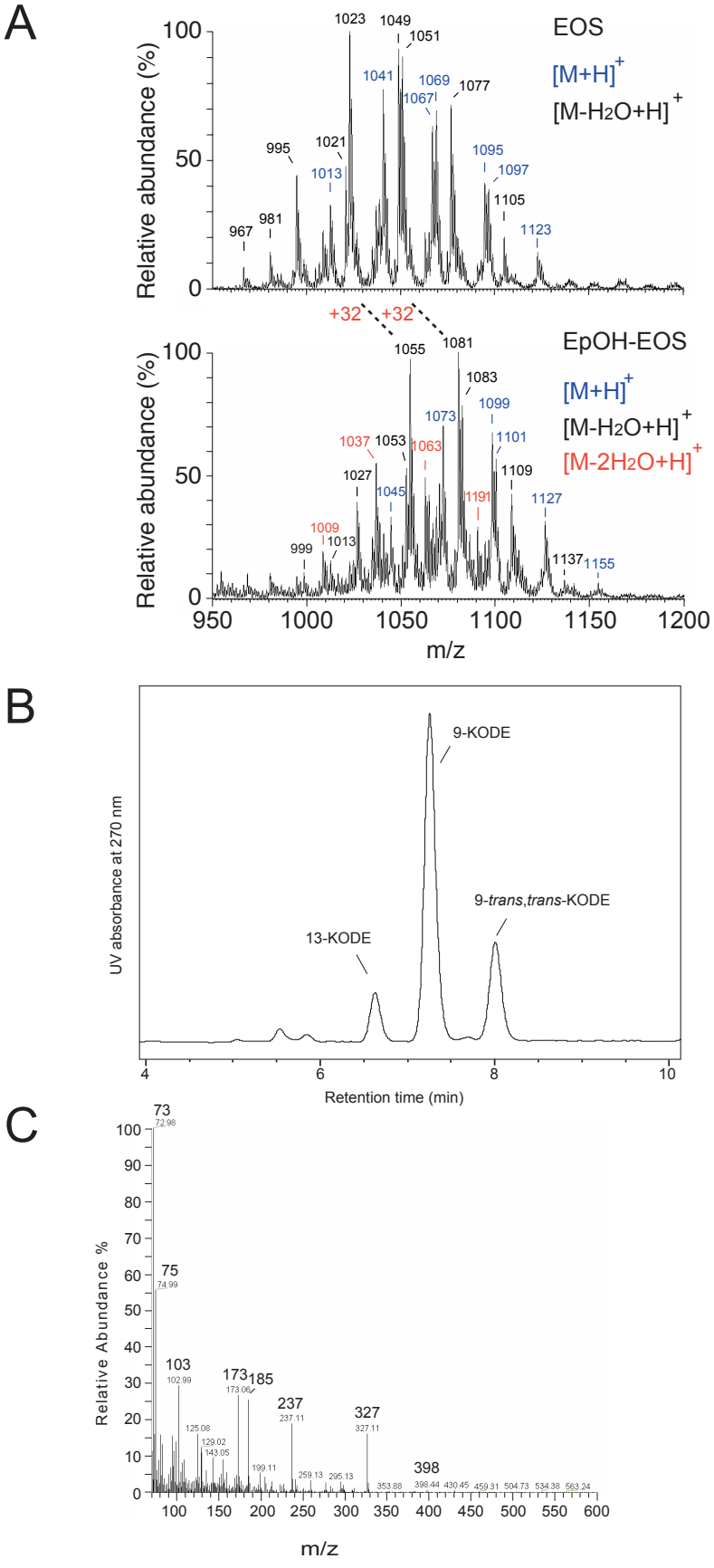

Fig. S2: Analysis of oxygenated EOS metabolites from pig epidermis. (**A**) [Top panel] Combined mass spectrum of EOS. [Bottom panel] Combined mass spectrum of epOH-EOS. (**B**) SP-HPLC analysis of KODE methyl esters transesterified from KODE-EOS. (**C**) GC-MS analysis of the TMS derivative of the major epOH methyl ester transesterified from epOH-EOS. For interpretation of the prominent ions, see Fig. S1E.

Figure S3

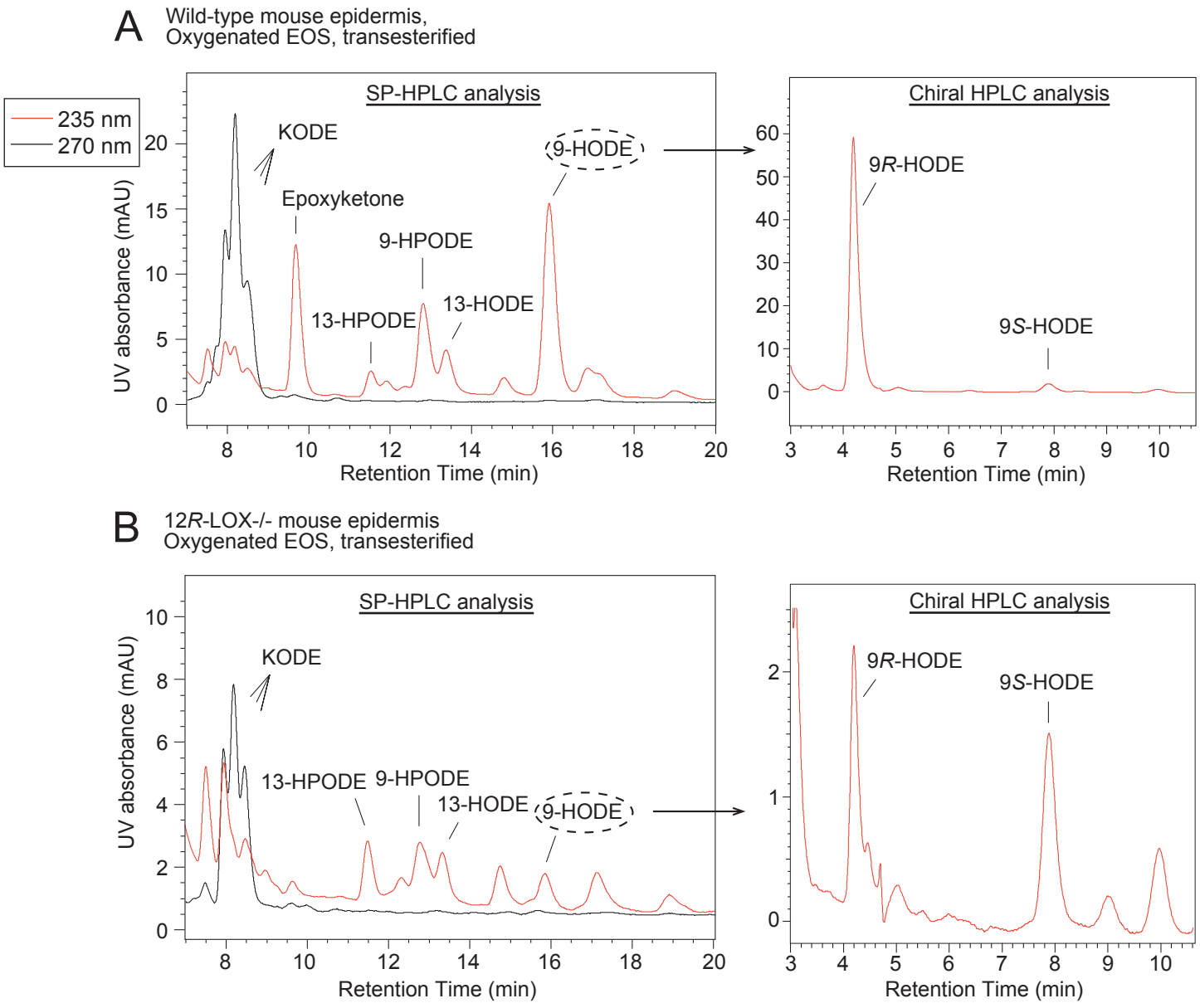

Fig. S3: Analysis of transesterified oxygenated EOS metabolites (HODE-EOS and KODE-EOS) from wild-type mouse epidermis (**A**) **and from 12R-LOX-/- mouse epidermis (B).** SP-HPLC analysis of KODE and epOH methyl esters tranesterified from the LOX product peak shown in Fig. 4A. Note that very little epoxy-ketone was recovered due to its instability under the alkaline conditions used for transesterification. 9-HODE methyl ester was collected and further analyzed by chiral HPLC (right panel). Identical aliquots were injected in this wild-type vs. 12R-LOX-/- comparison. Shown are representative chromatograms from three independent experiments on the same aliquots of the extract from three sets of wild-type and 12R-LOX-/- littermates.

Figure S4

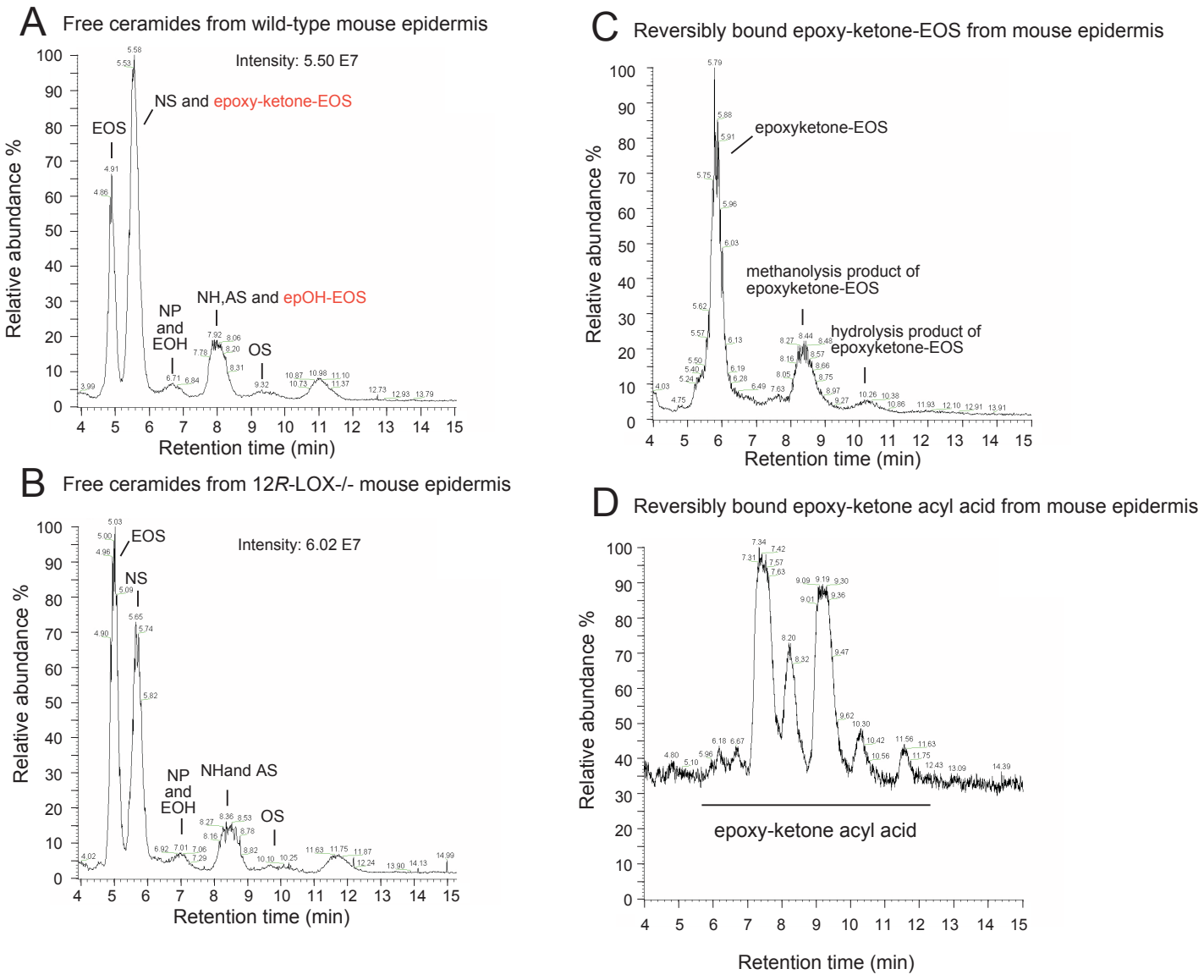

Fig. S4: Analysis of free and reversibly bound lipids from mouse epidermis. (**A**) and (**B**): Total ion current of SP-HPLC-APCI-MS analysis of free ceramides from wild-type and 12R-LOX-/- mouse epidermis respectively. The same aliquot was injected in this wild-type vs. 12R-LOX-/- comparison. (**C**) Total ion current of SP-HPLC-APCI-MS analysis of reversibly bound epoxy-ketone-EOS from wild-type mouse epidermis. (**D**) Total ion current of RP-HPLC-ESI-MS analysis of reversibly bound epoxy-ketone acyl acid from wild-type mouse epidermis.

(Figure S4 contd on next page)

(**E**) Mass spectrum of EOS from mouse epidermis. (**F**) Mass spectrum of free epoxy-ketone-EOS from mouse epidermis. (**G**) Mass spectrum of free epOH-EOS from mouse epidermis. Note the pattern similarity between this spectrum and the spectrum of free epoxy-ketone-EOS in (**F**). (**H**) Mass spectrum of reversibly bound epoxy-ketone-EOS from mouse epidermis. (**I**) Mass spectrum of reversibly bound epoxy-ketone acyl acid from mouse epidermis.

Figure S4-continued

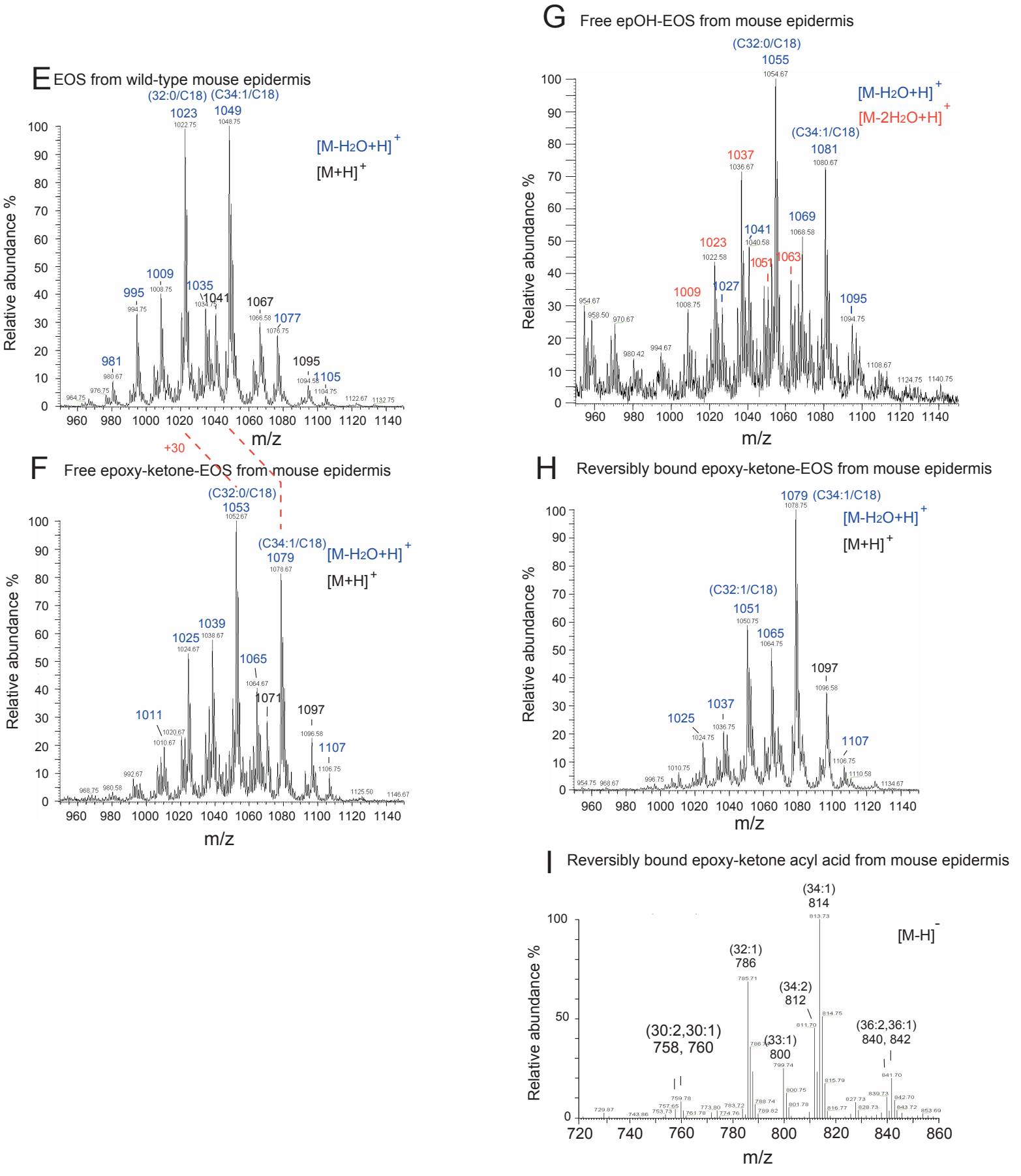

Figure S5

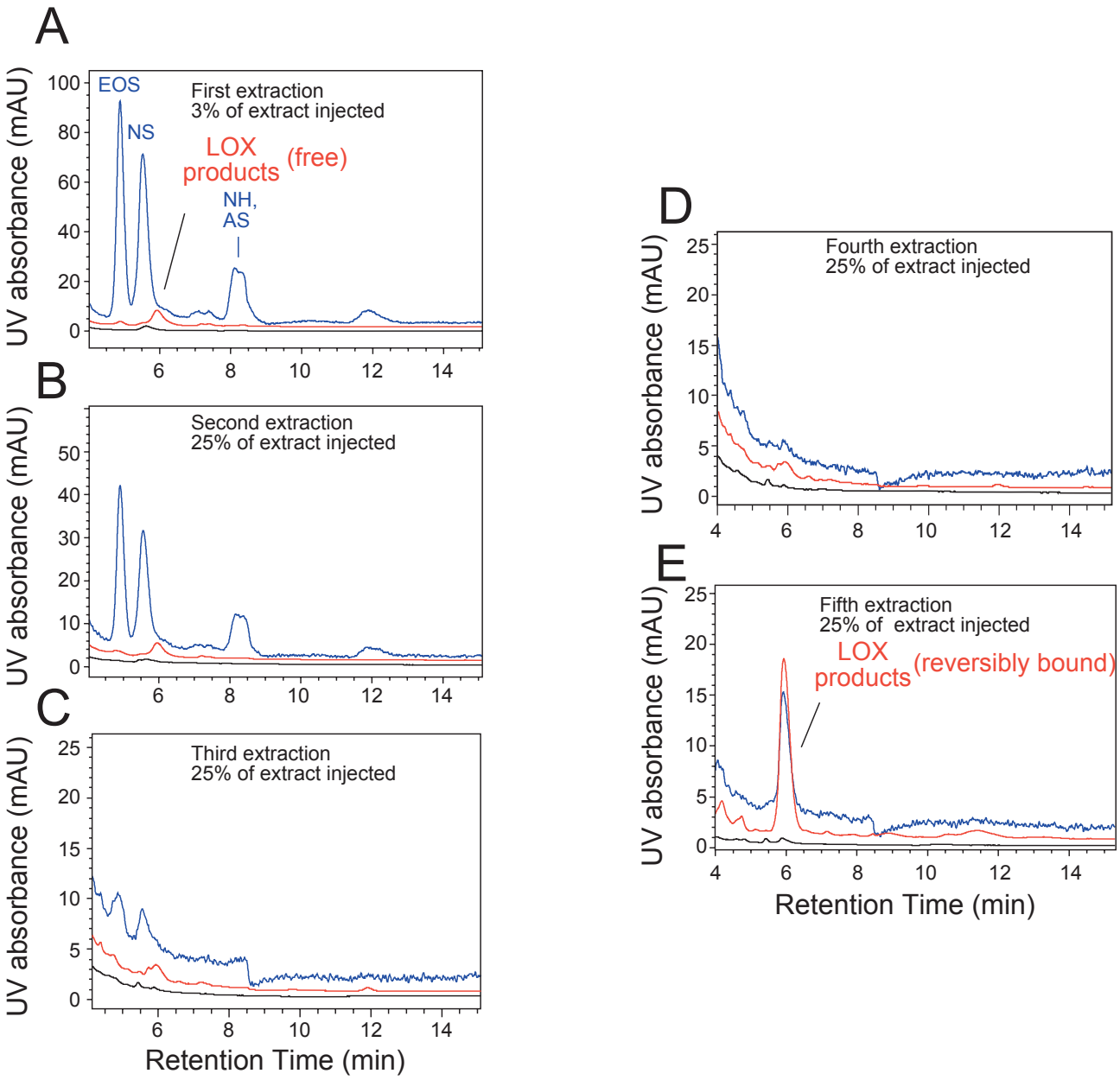

Fig S5: Stepwise extraction of mouse epidermis reveals lipids reversibly bound to proteins. (**A**)-(**D**): First to fourth sonication and extraction by chloroform:methanol (1:1 for A and B, or 2:1 for C and D, v/v) at 0 °C. Sonication lasted for 20 min each time (20 s sonication followed by 20 s interval). After each extraction, the organic phase was removed from the protein pellet by centrifugation. (**E**): A final soak of the protein pellet in chloroform:methanol (1:1, v/v) at room temperature overnight. For the first extraction, 3% of total extract was injected onto HPLC; for the next four extractions, 25% of total extract was injected. This experiment used epidermis isolated from two neonatal (P0) BALB/c mice.

Figure S6

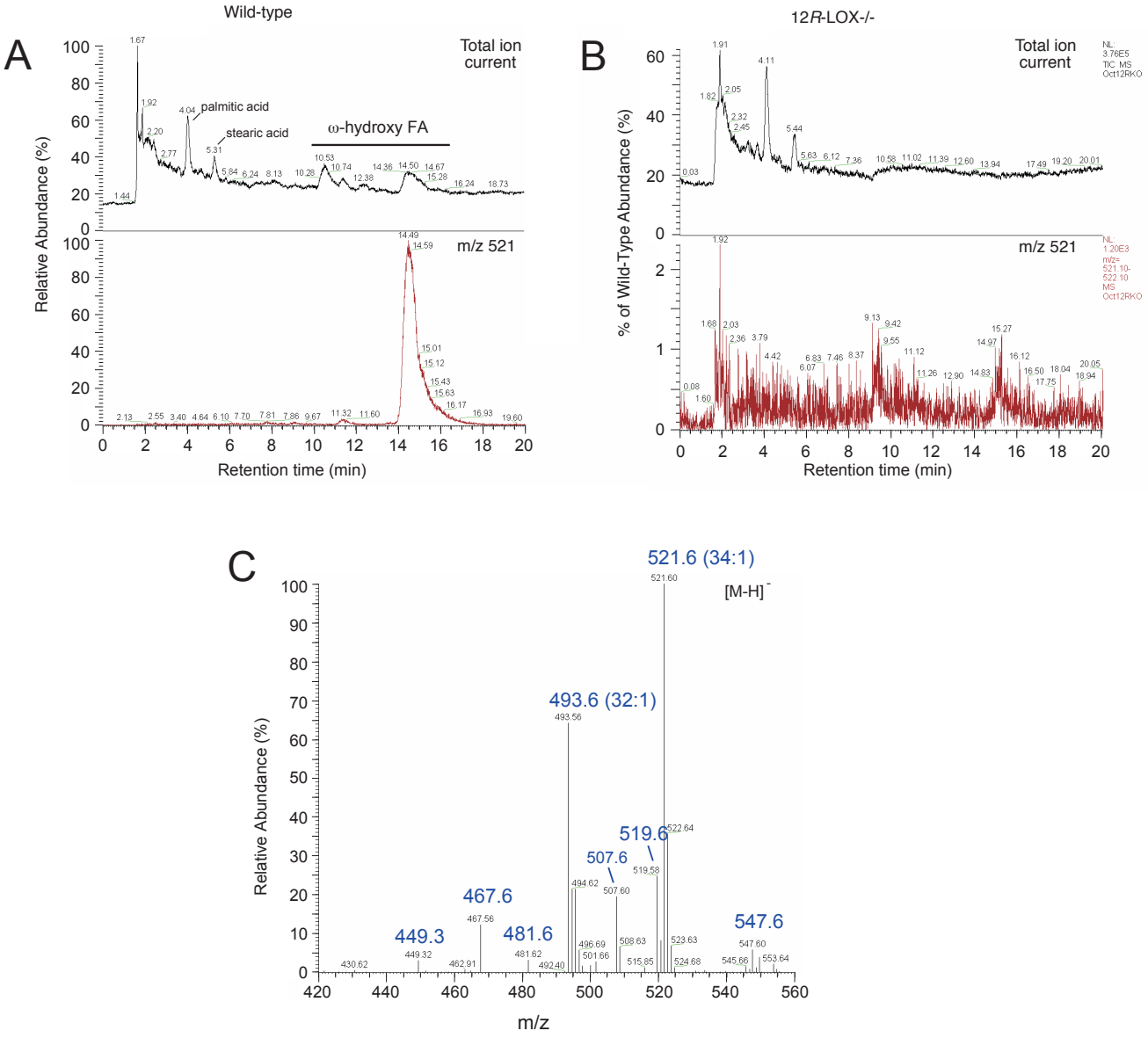

Fig. S6: Analysis of covalently bound FA and ω-hydroxy VLFA from mouse epidermis. (**A**) and (**B**): Total ion current of RP-HPLC-ESI-MS analysis of covalently bound lipids from wild-type and 12R-LOX-/- mouse epidermis respectively. The covalently bound lipids was recovered from mild alkaline hydrolysis of exhaustively extracted protein pellets. (**C**) Combined mass spectra of ω-hydroxy VLFA from wild-type epidermis.

Table S1. ^{1}H-NMR spectrum of 9*R*,10*R*-trans-epoxy-10*E*-13*R*-hydroxy-octadecenoate methyl ester. The spectrum (600 MHz) was acquired at room temperature in d_6-benzene solvent.

This epoxyalcohol is formed by eLOX3 reaction with 9*R*-HPODE esters, it occurs naturally in pig and mouse epidermis as EpOH-EOS, and it corresponds to the first of four 9,10-*trans*-epoxy-13-hydroxy isomers formed by hematin treatment of 9-HPODE (see Fig 3C, main text).

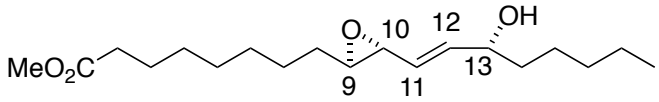

Chemical shift	Multiplicity	Assignment, coupling constant
5.79	dd	H12 $J_{11,12}$ = 15.5 Hz, $J_{12,13}$ = 5.9Hz
5.43	ddd	H11 $J_{11,12}$ = 15.5 Hz, $J_{10,11}$ = 7.8Hz, $J_{11,13}$ = 1.3 Hz
3.88	m	H13
3.37	s	-OCH_3
2.98	dd	H10 $J_{9,10}$ = 2.0 Hz, $J_{10,11}$ = 7.8 Hz
2.67	dt	H9 $J_{9,10}$ = 2.0 Hz, $J_{8,9}$ = 5.5 Hz
2.11	t	H2
1.53	quintet	H3
1.35-1.45	m	H8, 14
1.25	m	H17
1.0-1.30	m	H4, H5, H6, H7, H16, H15
0.95	d	OH (at C13)
0.88	t	H18